Macromolecules **2008,** *41,* 1685−1692

Synthesis of POSS−Methyl Methacrylate-Based Cross-Linked Hybrid Materials

Elda Markovic,*[,†] Stephen Clarke,[†] Janis Matisons,[†] and George P. Simon[‡]

Nanomaterials Research Group, School of Chemistry, Physics and Earth Science, Flinders University, Bedford Park, GPO Box 2100, South Australia, and Department of Materials Engineering, Monash University, Clayton, Victoria, Australia 3800

Received September 19, 2007; Revised Manuscript Received December 12, 2007

ABSTRACT: A series of $\mathrm{POSS}^{(\mathrm{PEG})n=2-6}$ macromonomers were further functionalized by reaction with methacryloyl chloride and then polymerized with methyl methacrylate to produce a series of hybrid materials where the amounts of $\mathrm{POSS}^{(\mathrm{PEG})n=2-6}$ used as cross-linkers varied from 0.1 to 0.5 mol %. Thermal investigations using TGA and DSC techniques revealed that both POSS concentrations and PEG chain length play important roles in defining structure−property relationships. Incorporation of POSS always increased thermal stability. Although the POSS is a bulky and multifunctional cross-linker, glass transitions did not always increase. In some instances bulkiness of the group created free volume and chain separation, which led to a reduction in the glass transition temperature.

Introduction

The increase of research into hybrid polymer−inorganic nanocomposites showing enhanced properties has been a focus of investigations for the past decade.[1] Significant enhancement of thermal, mechanical, and physical properties of hybrid materials can be achieved by incorporating a variety of nanofillers, such as carbon nanotubes, layered silicates, and polyhedral oligomeric silsesquioxanes (POSS) into many common plastics.[2−4] Unlike conventional inorganic fillers, POSS nanofillers offer the advantage of monodisperse size, low density, and synthetically well-controlled functionalities. The incorporation of nanosized POSS macromers into polymers has produced significant improvement in thermal and oxidative resistance as well as a reduction in the flammability of several POSS-based polymers, these systems then being suitable candidates in high-temperature and fire-resistant applications.[5−7] POSS compounds can be incorporated into polymers by blending, copolymerization, or grafting. POSS−polymer blends do create interesting materials, but microphase separation may occur, decreasing possible advantages connected with nanoscale incorporation.

The simplicity of introducing reactive functionalities to POSS moieties makes these compounds favored over other nanofillers as they can be incorporated in a controlled manner into polymer matrices via copolymerization or grafting. Nanosized POSS core molecules, with diameter dimensions between 0.6 and 1.2 nm and possessing a number of spaced polymerizable end groups, are often incorporated into common plastics by covalent bonding to the polymer matrix. Organic polymers can be reinforced with POSS by attaching single or multiple polymerizable groups to the POSS cage. If multifunctional POSS molecules are used as nanosized fillers in the molecular building-block approach to the design of organic−inorganic hybrid materials, the POSS cages become cross-linking points in the network. Polyhedral octasilsesquioxane (POSS) macromonomers bearing various polymerizable organic groups can thus be covalently added to polymeric matrices and function as nano-cross-linkers. These POSS macromonomers are generally synthesized through the hydrosilylation reaction of Si−H functional group and unsaturated compounds that either have, or can be further functionalized into, polymerizable groups.[8] In addition, the synthesis of POSS monomers can be accomplished by the hydrolytic condensation of trifunctional monomers $\mathrm{RSiX_3}$, where R is a functional organic substituent and X is a highly reactive substituent such as Cl, alkoxy, or ethoxy.[9] Examples of polymers or networks containing POSS units covalently incorporated are methacrylate,[10−12] epoxy,[13−17] vinyl,[18−22] polyamines,[23,24] and polyurethane.[25]

Table 1. Molar Ratio of OMPS and MMA Used for Polymerizations

$\mathrm{POSS}^{(\mathrm{PEG})n=2-\mathrm{Meth}}$ (mol %)	$\mathrm{POSS}^{(\mathrm{PEG})n=2-\mathrm{Meth}}$ (g/mmol)	MMA (g/mmol)	benzoyl peroxide (mmol)
0	0	5 (44.0)	0.038
0.1	0.1365 (0.049)	5 (44.0)	0.038
0.2	0.2731 (0.099)	4.99 (49.8)	0.036
0.3	0.2048 (0.075)	2.495 (24.9)	0.018
0.5	0.3400 (0.120)	2.49 (24.8)	0.013

This paper describes the synthesis of hybrid inorganic−organic POSS-containing, cross-linked methacrylate matrices. $\mathrm{POSS}^{(\mathrm{PEG})n=2-6}$ macromonomers that we previously reported[26] were further functionalized by reaction with methacryloyl chloride and copolymerized with methyl methacrylate, resulting in a series of new hybrid materials where the amounts of $\mathrm{POSS}^{(\mathrm{PEG})n=2-6}$ used as cross-linkers could be varied from 0.1 to 0.5 mol %. The properties of these hybrid materials were then examined by TGA and DSC and structure−property correlations made.

Experimental Section

Materials. Ethylene glycols, allyl bromide, 2,2,4-trimethylpentane, ferric chloride, methanol, toluene, hydrochloric acid, sodium dodecyl sulfate, trichlorosilane, potassium carbonate, calcium chloride, pentane, cyclohexane, and Karstedts catalyst, [Pt(dvs)], were obtained from Aldrich Chemical Co. Octa(dimethylsiloxy)-silsesquioxane ($\mathrm{Q_8M_8^H}$) was purchased from Hybrid Plastics. Toluene (99.5%) was purchased from Fluka, dried over $\mathrm{CaH_2}$, and then distilled prior to use (Na/benzophenone).

Characterization Methods. NMR spectra were obtained on a Varian 300 NMR. Samples for ^{1}H NMR and ^{13}C NMR were

---

* Corresponding author: Ph 61 8 8201 3537; Fax 61 8 201 5571; e-mail elda.markovic@flinders.edu.au.

[†] Flinders University.

[‡] Monash University.

10.1021/ma702103z CCC: $40.75

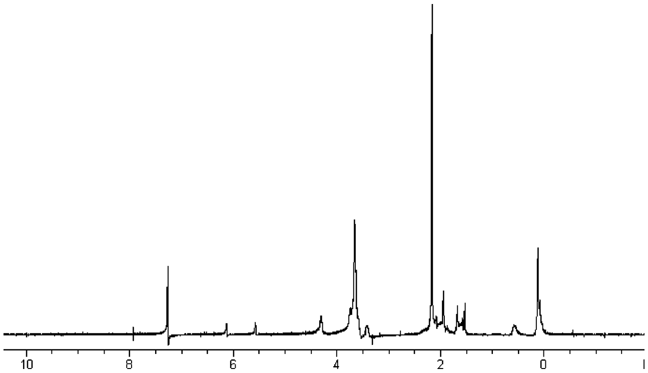

Figure 1. ^{1}H NMR of OMPS.

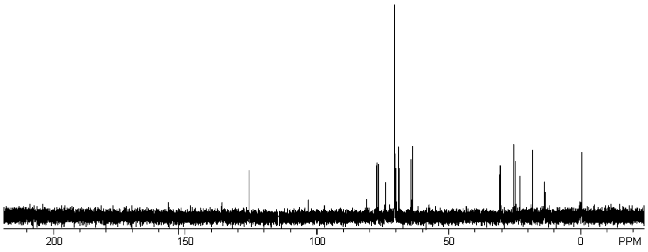

Figure 2. ^{13}C NMR spectrum of OMPS.

prepared in $CDCl_3$. TMS (tetramethylsilane) was used as an internal standard for ^{29}Si NMR. Thermogravimetric analysis (TGA) and differential scanning calorimetry (DSC) were carried out on a TA Instruments TGA 2950 thermogravimetric analyzer and a TA-DSC 2920, respectively.

Synthesis of Octakis(methacryldiethoxypropyldimethylsilyl)-octasilsesquioxane (OMPS). Methacryloyl-functional Q_8M_8−PEG (OMPS) macromonomers were synthesized from Q_8M_8−PEGs. Synthesis of octakis(methacryldiethoxypropyldimethylsilyl)octasilsesquioxane (OMPS) is described as a representative example. Octakis(hydroxydiethoxypropyldimethylsilyl)octasilsesquioxane, $Q_8M_8^{(PEG)n=2}$ (1.5366 g, 7.029×10^{-4} mol), was placed in a 100 mL three-neck flask equipped with a magnetic stirrer, reflux condenser, dropping funnel, and a nitrogen purge. CH_2Cl_2 (20 mL) was added to dissolve $Q_8M_8^{(PEG)n=2}$ and stirred for 10 min. Triethylamine (0.804 mL, 5.769×10^{-3} mol) was added, and the reaction mixture was cooled to −78 °C. Methacryloyl chloride (0.6 mL, 6.76×10^{-3} mol) was dissolved in CH_2Cl_2 and added dropwise via a dropping funnel. The formation of a pink precipitate and evolution of HCl confirmed the reaction progress. The reaction mixture was stirred at −78 °C for 1 h and then for 2 h at room temperature. The mixture was filtered and the filtrate transferred to a separating funnel. The filtrate was washed with deionized water, 0.5 N NaOH, and saturated NaCl. The organic phase was separated and dried over sodium sulfate, filtered, and evaporated. The product octakis(methacryldiethoxypropyldimethylsilyl)octasilsesquioxane was isolated as a yellow, slightly viscous oil. All other OMPS bearing various PEG chains were synthesized following the same procedure. The products were characterized by FT-IR, ^{1}H NMR, ^{13}C NMR, ^{29}Si NMR, TGA, and DSC.

FT-IR (cm^{-1}): $\nu = 2960$ cm^{-1} (aliphatic CH_2), 2875 cm^{-1} (O−CH_2−CH_2), 1720 cm^{-1}(C=O), 1107 s (O−Si−O), 885 s (O−Si−H).

^{1}H NMR (ppm) (300 MHz, $CDCl_3$): δ 6.14 (s 1H $CH_3C{=}C\mathit{H}_2$) 5.58 (s 1H $CH_3C{=}C\mathit{H}_2$) 4.25 (t 2H $OCH_2C\mathit{H}_2OCOCCH2$) 3.61−3.65 (m 6H $C\mathit{H}_2C\mathit{H}_2OC\mathit{H}_2$), 3.40 (t 2H $SiCH_2CH_2C\mathit{H}_2$), 2.18 (s 3H $OCOCHCH_2C\mathit{H}_3$) 1.60 (m 2H $SiCH_2C\mathit{H}_2CH_2$), 0.56 (t 2H Si-$(CH_3)_2C\mathit{H}_2CH_2CH_2$), 0.13 (s 6H Si$(C\mathit{H}_3)_2$).

^{13}C NMR (ppm) (300 MHz, $CDCl_3$): δ 166 ($O\mathit{C}OCCH_2CH_3$) 138 ($OCO\mathit{C}CH_2CH_3$) 130 ($OCOC\mathit{C}H_2CH_3$) (69.95−73.36 4C ($\mathit{C}H_2\mathit{C}H_2O\mathit{C}H_2\mathit{C}H_2$), 61.61 ($\mathit{C}H_2OH$), 22.81 ($OCOCCH_2\mathit{C}H_3$) ($Si(CH_3)_2CH_2\mathit{C}H_2CH_2$), 8.05 ($Si\mathit{C}H_2CH_2CH_2$).

^{29}Si NMR (ppm) (300 MHz, TMS): 13.24 (−O*Si*$(CH_3)_2$), −109.22 (*Si*O_4).

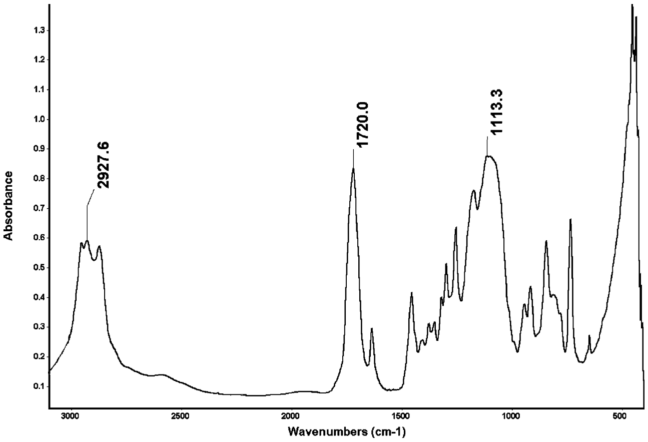

Figure 3. FT-IR spectrum of OMPS.

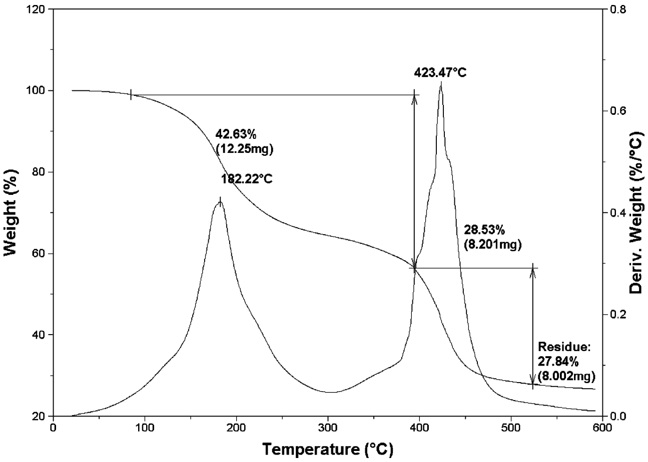

Figure 4. TGA thermogram of OMPS.

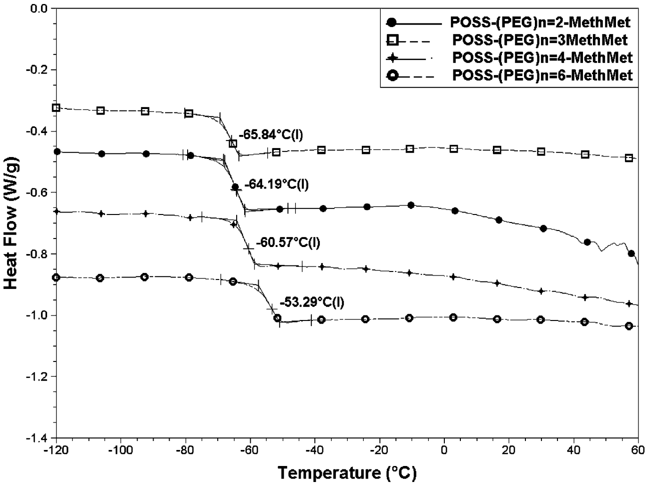

Figure 5. Glass transition temperatures for OMPS compounds.

Polymerizations of Methacryloyl-Functional POSS−PEGs (OMPS) with Methyl Methacrylate. Bulk polymerizations at various mole fractions of methacryloyl-functional POSS−PEGs were carried out. The polymerization of octakis(methacryldiethoxypropyldimethylsilyl)octasilsesquioxane (OMPS) with methyl methacrylate monomer (MMA) is described here as an example. The 0.1 mol % hybrid of OMPS with MMA was prepared by dissolving OMPS (0.1365 g, 0.049 mmol) in MMA (5.23 mL, 48.95 mmol) in a 100 mL three-neck flask equipped with magnetic stirrer, reflux condenser, and a nitrogen purge. The initiator, dibenzoyl peroxide (0.0388 g), was added, and the reaction mixture stirred for 30 min under nitrogen at room temperature. The mixture was then transferred into a PTFE Petri dish, flushed with nitrogen, sealed,

Scheme 1. Synthesis of Octakis(methacryldiethoxypropyldimethylsilyl)octasilsesquioxane (OMPS)

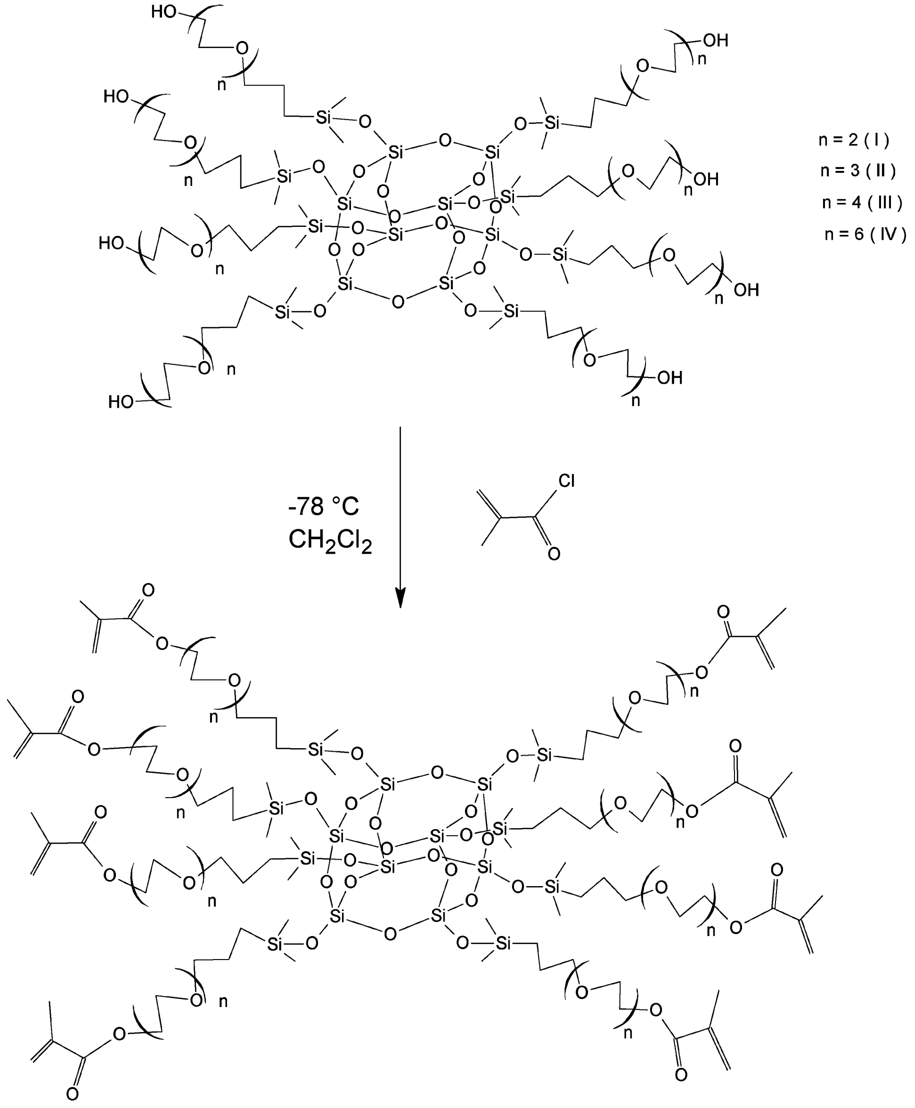

and left in the oven at 80 °C for 24 h. A series of hybrid materials were prepared, where the content of OMPS was varied from 0.1 to 0.5 mol %, for four different PEG chain length OMPS. Table 1 shows the amounts of monomer and POSS−PEGs used in the preparation of hybrid materials.

Results and Discussion

Synthesis of Octakis(methacryldiethoxypropyldimethylsilyl)-octasilsesquioxane (OMPS). Methacryloyl-functional Q_8M_8−PEG macromonomers (OMPS) were synthesized from previously reported $Q_8M_8^{(PEG)n=2-6}$.[26] A series of methacryloyl-functional POSS precursors that can be used for the synthesis of poly(methyl methacrylates) have been synthesized from octafunctional poly(ethylene glycol)-substituted POSS, $Q_8M_8^{PEG(n=2-6)}$, macromonomers in separate reactions (Scheme 1). The macromonomers were synthesized by two-step reactions. The first step employed the hydrosilylation reaction of Q_8M_8 with a series of allyl-functional poly(ethylene glycol)s.[26] The second step involved subsequent reaction with methacryloyl chloride to obtain methacryloyl-functional POSS macromonomers that were used in the polymerization reactions to obtain a series of three-component polymers, POSS−PEG−PMMA. Methacryloyl-functional POSS macromonomers, OMPS, were prepared from reactions of POSS−PEGs with methacryloyl chloride at −78 °C.

The materials were characterized by NMR, FT-IR, TGA, and DSC. Figure 1 shows the ^{1}H NMR spectrum of OMPS. The disappearance of the OH broad peak at δ 2.90 ppm indicated the completeness of esterification reaction. The appearance of the strong single peak at $\delta = 1.94$ ppm was attributed to the CH_3 moiety of the methacryloyl group, with two singlets at $\delta = 5.58$ and $\delta = 6.05$ attributed to methacryloyl protons, and this confirmed the synthesis of the methacryloyl-functional product.

Figure 2 shows ^{13}C NMR of OMPS. The peak at $\delta = 0.13$ ppm was attributed to the carbons of CH_3 next to the Si of the siloxane fraction of silsesquioxane cage, O−Si(CH$_3$)$_2$−CH$_2$−CH$_2$CH$_2$O). Peaks at $\delta = 13.71$ ppm are due to OSi(CH$_3$)$_2$−CH$_2$−CH$_2$CH$_2$O and at $\delta = 23.13$ ppm due to OSi(CH$_3$)$_2$−CH$_2$−CH$_2$CH$_2$O. Carbons between 65 and 75 ppm are due to the glycol part of the monomer. Carbonyl carbons from the methacryloyl (COC−CH$_2$═CH$_2$) group were found at 125 ppm.

Figure 3 shows the FT-IR spectrum of OMPS. The appearance of the peak at $\nu = 1722$ cm^{-1}, which is significant C═O stretching, as well as disappearance of the OH stretching of POSS−PEG at $\nu = 3407$ cm^{-1} confirmed the successful synthesis of the methacryloyl-functional POSS−PEG macromonomer. Peaks at $\nu = 2860$ cm^{-1} were assigned to the aliphatic O−CH$_2$−CH$_2$ glycol vibrations. A peak found at 1627

Table 2. Decomposition Temperatures of OMPS Compounds

$POSS^{-PEG}$	first decomp (°C)	second decomp (°C)	$POSS^{-PEG-Meth}$	first decomp (°C)	second decomp (°C)	calcd SiO_2	exptl SiO_2
$Q_8M_8^{(PEG)n=2}$	164	394	$Q_8M_8^{(PEG)n=2-Meth}$	182	423	28.7	26.7
$Q_8M_8^{(PEG)n=3}$	198	388	$Q_8M_8^{(PEG)n=3-Meth}$	182	423	25.17	23.3
$Q_8M_8^{(PEG)n=4}$	208	385	$Q_8M_8^{(PEG)n=4-Meth}$	180	428	22.9	20.2
$Q_8M_8^{(PEG)n=6}$	268	359	$Q_8M_8^{(PEG)n=6-Meth}$	184	434	18.4	15.4

Table 3. DSC Data for [$POSS^{(PEG)n=2-6}$] and OMPS [$POSS^{(PEG)n=2-6-Methac}$]

$POSS^{-PEG}$	T_g	$POSS^{-PEG-Meth}$	T_g
$Q_8M_8\ ^{(PEG)n=2}$	−82.88	$Q_8M_8\ ^{(PEG)n=2-Meth}$	−64.35
$Q_8M_8\ ^{(PEG)n=3}$	−79.96	$Q_8M_8\ ^{(PEG)n=3-Meth}$	−61.84
$Q_8M_8\ ^{(PEG)n=4}$	−70.36	$Q_8M_8\ ^{(PEG)n=4-Meth}$	−60.57
$Q_8M_8\ ^{(PEG)n=6}$	−66.97	$Q_8M_8\ ^{(PEG)n=6-Meth}$	−53.46

cm^{-1} was attributed to the C═C stretching of the methacryloyl group. Other characteristic peaks assigned to the silsesquioxane cage were also found: $\nu = 1093\ cm^{-1}$ due to the Si−O−Si asymmetric stretching, $\nu = 800-810\ cm^{-1}$ attributed to Si−CH_3 rocking, and $\nu = 550-560\ cm^{-1}$ attributed to the Si−O−Si bending signal.

Thermal gravimetric analysis (TGA) was employed to examine thermal decomposition of the OMPS macromonomers. TGA data of OMPS synthesized from $Q_8M_8^{(PEG)n=2}$ exhibited two decomposition steps (Figure 4). The TGA curve demonstrates a first onset of degradation at 182 °C, attributed to the organic fraction of the OMPS macromonomer. It is most likely that this decomposition represents degradation of the methacryloyl group and a fraction of the PEGs that surround the POSS cage. The second decomposition is attributed to further degradation of the organic fraction of the POSS macromonomer. This involves degradation of the rest of PEG fraction along with the CH_3 groups attached to the siloxane part of the POSS cage. The observed experimental residue of 26.7% is in reasonable agreement with the calculated value for the silica content of the silsesquioxane compound (Table 2).

Table 2 summarizes TGA data for all OMPS compounds. Decomposition temperatures for POSS−PEG materials are also shown for comparison. As Table 2 indicates, unlike their POSS−PEG counterparts, the OMPS materials exhibit very slight increase in their thermal decomposition temperatures with the increasing PEG chain length.

The glass transition temperature of methacryloyl-functional POSS macromonomers is higher than POSS−PEGs, which is attributed to the longer chains attached to POSS cage which decreases their mobility. However, there is also a correlation between an increase in the glass transition temperatures of the OMPS compounds and the lengths of their PEG chain fractions. As the chain length of the OMPS increases, there is also a noticeable increase in their glass transition temperatures (Figure 5 and Table 3), and this was also observed with the POSS−PEGs due to an increase in the molecular weight.

Synthesis of Hybrid POSS−PEG−PMMA Materials by Polymerization of Methacryloyl-Functional POSS−PEGs (OMPS) with Methyl Methacrylate. POSS-containing cross-linked poly(methyl methacrylate) hybrid materials were synthesized from methacryloyl-functional Q_8M_8 macromonomers by free radical bulk polymerization using benzoyl peroxide as catalyst (Scheme 2). Methyl methacrylate was polymerized in the presence of methacryloyl-functional POSS−PEG (OMPS) cross-linkers in amounts ranging from 0.1 to 0.5 mol % to prepare hybrid polymers (POSS−PEG−PMMA). A series of brittle colorless, transparent plastic sheets were prepared from all derivatives of methacryloyl-functional $Q_8M_8^{(PEG)n=2-6}$ macromonomers by varying the POSS content and hybrid materials, which were characterized by FT-IR spectroscopy. Figure 6 shows the FTIR spectrum of hybrid POSS−PMMA material.

Figure 6 shows FT-IR spectra of commercial PMMA (A) and POSS−PMMA (B) materials, which was used as a reference. It can be seen from the figure that both PMMA materials exhibit aliphatic CH_2 bands at 2957−2850 cm^{-1} and a strong band at 1720 cm^{-1}, attributed to a carbonyl (C═O) stretching mode along with other bending and stretching mode peaks that were observed in the range of 1160−1452 cm^{-1}. However, the signals at 1085−1100 cm^{-1} as well as those at 550−560 cm^{-1}, which were attributed to Si−O−Si stretching and bending modes, respectively, found only in the FT-IR spectrum of the hybrid POSS−PMMA materials indicated the presence of POSS cages in the hybrid polymers.

TGA Study of POSS−PEG−PMMA. Thermal decomposition of hybrid POSS−PMMA materials was studied by TGA. Figure 7 shows TGA thermograms of the [$Q_8M_8^{(PEG)n=2}$]−PMMA hybrid materials with varying concentrations of OMPS at a heating rate of 10 °C/min. TGA thermograms of a series of PMMA materials containing various POSS concentrations were compared with a sample of neat poly(methyl methacrylate). It has been reported previously that polymers modified with polyhedral silsesquioxanes exhibit greater decomposition temperatures.[27] This property was reportedly connected to the ceramic nature of the silsesquioxane component, that creates a glassy layer during pyrolysis, which slows the rate of diffusion of decomposition gases. For example, decomposition temperatures of poly(4-methylstyrene) or polystyrene were increased by more than 50 °C by the incorporation of 20−40 wt % silsesquioxanes into the polymer matrices.[27−29] Also, recently reported synthesis of poly(4-vinylpyridine) nano-cross-linked by POSS, where POSS content was up to 55 wt %, showed that the increase in POSS concentration significantly improved thermal stability of these materials.[30] Such an "insulation effect" by well-dispersed POSS cubes on the thermal stability of the hybrid materials has also been reported in fully exfoliated polymer−clay nanocomposite hybrid materials.[31,32]

In this work, a poly(methyl methacrylate) network was generated by copolymerization of the very low mol % of octafunctional POSS species with methyl methacrylate monomer. As shown in Figure 7, the thermal stabilities of hybrid materials were indeed significantly enhanced with increasing POSS component, in spite of its very low concentration. Figure 7 shows the thermograms of hybrid POSS−PEG−PMMA materials prepared from octafunctional POSS with the shortest PEG chains [$Q_8M_8^{(PEG)n=2}$]−PMMA. The major decomposition for PMMA with 0.5 mol % POSS content has been shifted to 400 °C, relative to neat PMMA (350 °C).

For comparison, the TGA thermograms of the series of hybrid materials prepared from POSS with longer PEG chains [$Q_8M_8^{(PEG)n=6}$]−PMMA are shown in Figure 8.

In the case of these hybrids, however, the onset of decomposition was shifted to higher values than those materials that incorporated POSS with shorter PEG chains, [$Q_8M_8^{(PEG)n=2}$]−PMMA. Figure 8 shows that, even for a low content of POSS (0.1 mol % [$Q_8M_8^{(PEG)n=6}$]−PMMA, there is a significant shift in decomposition temperature (≈20 °C), increasing progressively

Scheme 2. Polymerization of Methyl Methacrylate Using OMPS as Cross-Linkers

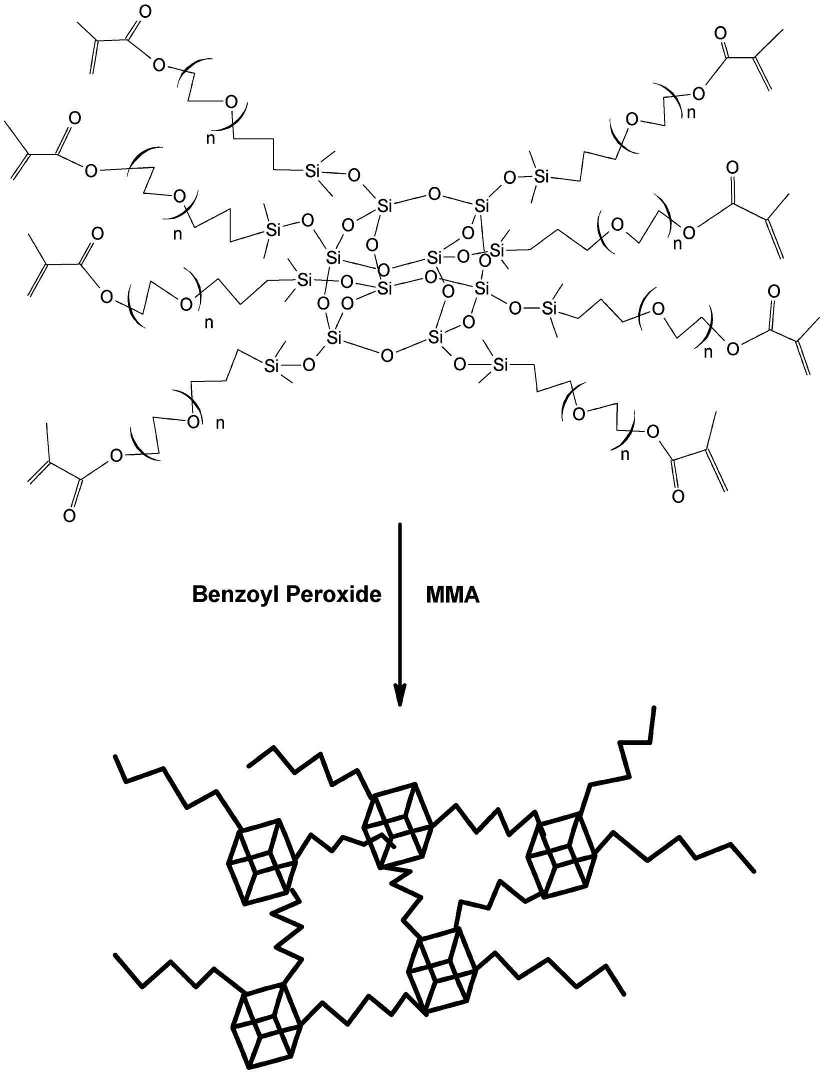

as the POSS concentration increases. This improvement in thermal stability is attributed to the nanoscale dispersion of POSS cages, surrounded by various chain length ethylene glycols in poly(methyl methacrylate) matrix. It appears that the thermal decomposition of poly(methyl methacrylate) is significantly suppressed by incorporation of a well-dispersed octafunctional POSS cage, surrounded by long PEG chains. Thermal properties of all hybrid polymers prepared in this work are summarized in Table 4.

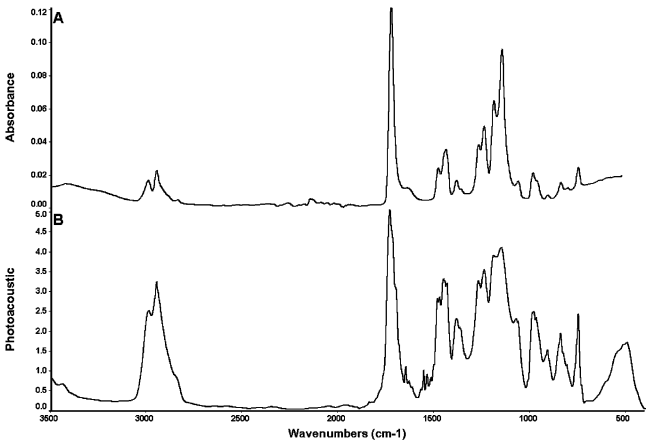

Figure 6. FT-IR spectra of (A) PMMA and (B) POSS−PEG−PMMA hybrids.

Table 4 shows the decomposition temperatures for all hybrid materials. It is clear from both thermograms (Figures 7 and 8) and Table 4 that degradation of hybrid materials takes place as a two-step decomposition process. The temperature of the first step generally increases with increasing mole percentage of POSS−PEG−PMMA. However, a decrease was noted for materials having 0.5 mol % of POSS−PEG incorporated into the hybrid structures and with (PEG)*n*, where *n* > 2. In Figure

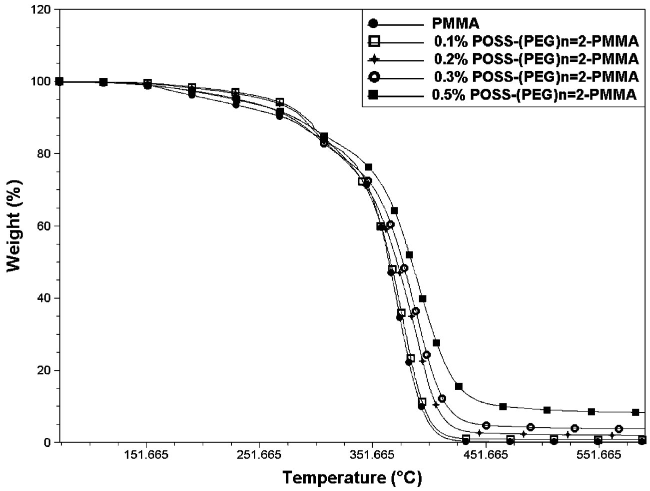

Figure 7. TGA thermograms of $[Q_8M_8^{(PEG)n=2}]$−PMMA.

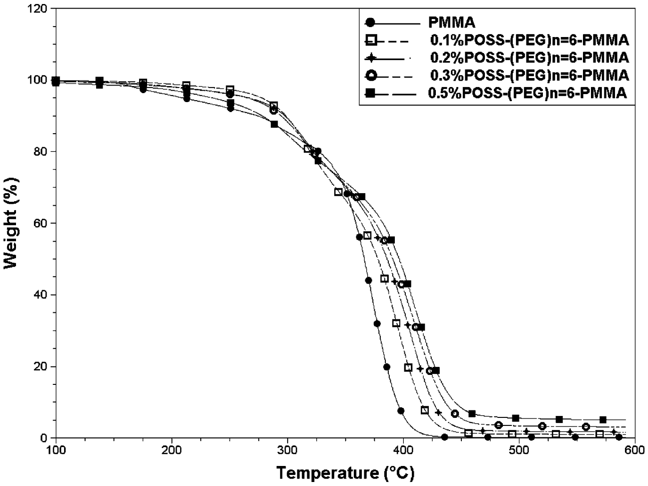

Figure 8. TGA thermograms of $[Q_8M_8^{(PEG)n=6}]$−PMMA.

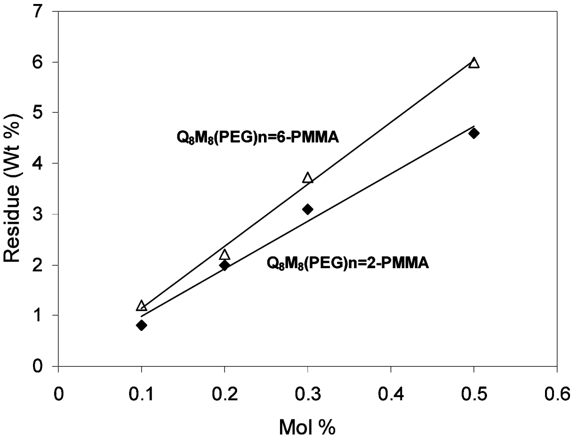

Figure 9. Plot of residue wt % of POSS−PEG−PMMA vs mol %.

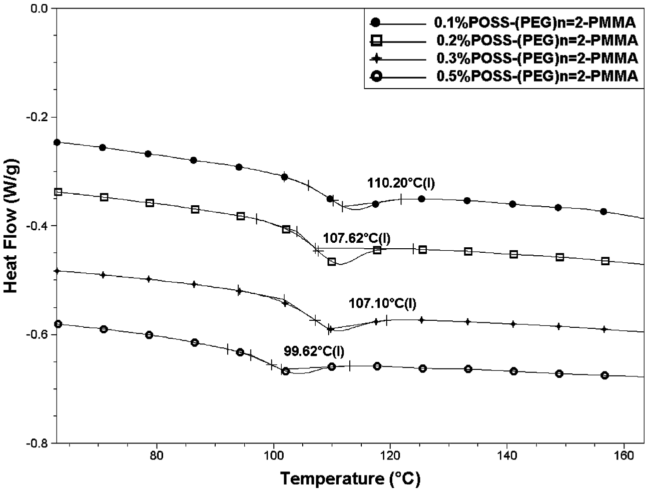

Figure 10. DSC thermograms of of $[Q_8M_8^{(PEG)n=2}]$−PMMA.

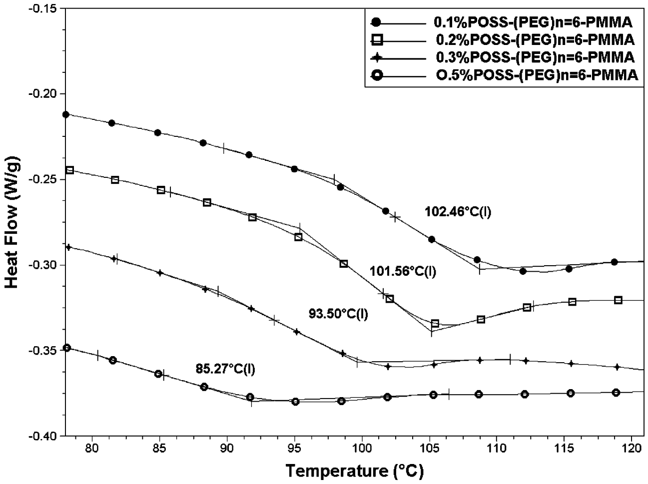

Figure 11. DSC thermograms of $[Q_8M_8^{(PEG)n=6}]$−PMMA.

9, the residue left after 550 °C was plotted as a function of mol % for the two series of hybrid materials: $[Q_8M_8^{(PEG)n=2}]$−PMMA and $[Q_8M_8^{(PEG)n=6}]$−PMMA. It can be seen from Figure 9 that the residue increased with greater mole percentages of the POSS−PEG concentration in the POSS−PEG−PMMA materials. It is also higher for the hybrids prepared from the $[Q_8M_8^{(PEG)n=6}]$−PMMA than for those prepared from $Q_8M_8^{(PEG)n=2}$−PMMA.

DSC Studies of POSS−PEG−PMMA. To further study the effect of the incorporation of octafunctional POSS−PEG into the poly(methyl methacrylate) matrix, each series of POSS−PEG−PMMA materials were investigated by DSC. DSC studies confirmed that both the increase in POSS−PEG concentration and the PEG chain length affected thermal behavior of these hybrid materials. For comparison, the DSC data of two series of the hybrid materials prepared from macromonomers possessing shorter and longer PEG chains around POSS cages are shown in Figures 10 and 11.

No exothermic peaks appeared in the thermograms, which indicated that no reactive methyl methacrylate monomer residues were present in the nanocomposite materials, confirming that the degree of the reaction was high in all cases. However, interestingly, Figures 10 and 11 demonstrate that the *increase* in POSS−PEG concentrations for the hybrid nanomaterials *lower*s the glass transition temperatures (T_g) of the hybrids. Glass transition temperature observed for pure PMMA prepared by the same method was 110 °C. Figure 10 shows the DSC thermograms of 0.1−0.5 mol % hybrids prepared from the octafunctional POSS−PEG with shortest PEG chains $(Q_8M_8^{(PEG)n=2}]$−PMMA. This effect was observed to be more pronounced for materials prepared from POSS−PEG with longer PEG chains $[Q_8M_8^{(PEG)n=6}]$−PMMA. These results confirmed that the addition of the POSS−PEG macromonomers, as nano-cross-linkers, in poly(methyl methacrylate) matrix reduces the T_g of the hybrid material. This DSC data demonstrates altered thermal behavior compared to materials studied previously, where incremental POSS incorporation initiated increase in glass transition temperatures. Recent DSC studies, for example, have reported that POSS-containing poly(methyl methacrylate) copolymers demonstrated an increasing T_g with increasing POSS concentrations in the polymer.[11] However, in the case of hybrid poly(methyl methacrylates), incorporating these nanosized POSS−PEG cross-linkers at very low concentrations of POSS−PEG cages increased T_g, which then decreased at higher POSS−PEG contents. The decrease in T_g of the three-component POSS−PEG−PMMA hybrids is most likely due to an increase in free volume accompanying a high level of dispersion of the POSS cross-linking monomers within the polymer matrix. Similar observations were reported for epoxy/POSS nanocomposites with 25% of POSS content showing a lower T_g compared to the neat epoxy resin.[33,34] This behavior was attributed to the separation of polymer chains caused by bulkiness of POSS cages, also mentioned by Xu et al.[35] and Haddad et al.,[36] where chain separation additionally prevented interchain hydrogen bonding in these epoxy systems.[16] DSC studies of poly(hydroxystyrene-*co*-vinylpyrolidone-*co*-isobutylstyryl polyhedral oligosilsesquioxane) demonstrated

Table 4. Decomposition Temperatures of Hybrid POSS−PEG−PMMA Materials

POSS−(PEG)*n*=2−6−PMMA	mol % of OMPS in PMMA	first decomp (°C)	second decomp (°C)	residue (wt %)
POSS−(PEG)*n*=2−PMMA	0.1	292	375	0.8
	0.2	285	378	2
	0.3	293	384	3.1
	0.5	295	392	4.6
POSS−(PEG)*n*=3−PMMA	0.1	293	382	1.3
	0.2	302	393	2.7
	0.3	302	394	3.2
	0.5	294	389	5
POSS−(PEG)*n*=4−PMMA	0.1	301	400	2.4
	0.2	312	402	2.9
	0.3	322	386	3.3
	0.5	303	395	4.9
POSS−(PEG)*n*=6−PMMA	0.1	313	395	1.4
	0.2	313	408	2.2
	0.3	312	412	3.7
	0.5	302	411	6

lower T_g of the hybrids as the POSS concentration increased[37] and it was suggested that interactions between the copolymers reduced the origial dipole−dipole interaction within the polymers. It is not only the inclusion of the POSS units themselves that can reduce T_g. In the system of Kim et al.[38] the flexible siloxane spacer unit attached to the two of the apexes of the POSS cube led to a more flexible molecular environment, thus lowering the T_g. In the case of POSS−PS hybrids, where monofunctional styryl-POSS with seven inert *i*-Bu groups was polymerized with styrene monomer, it was observed that the *i*-Bu−POSS played a plasticizer-like effect on the final structure, leading to a monotonic decrease of the glass transition temperature with increasing POSS concentration. In this case, the copolymers have the polystyrene backbone randomly branched by *i*-Bu−POSS, such that it increased the distance between adjacent backbone chains which lead to a higher free volume. Consequently, the chain mobility is greater, and *i*-Bu−POSS assumes a plasticizing role. In addition, morphological studies revealed that *i*-Bu−POSS was well dispersed in the polystyrene matrix at a molecular level. Despite this mixing, the interchain interactions between *i*-Bu−POSS and polystyrene are due to weak van der Waals forces, and this leads to lower T_g due to a reduction in entanglement density. Another possible explanation for the lower T_g of POSS−PS is that the significant free volume of the POSS molecule created a steric barrier, increasing the resistance to torsional rotation about σ bonds in the polymer backbone.[39]

In summary, the observed behavior of hybrid POSS−PEG−PMMA materials can be explained by either the bulky POSS−PEG cross-linker significantly increasing the free volume to a greater degree for POSS units with longer PEG chains and/or the POSS−PEG having an obstructing effect on PMMA chain motions. It is most likely that the combination of both factors accounts for the decrease of T_g of the hybrid materials with an increase in POSS−PEG concentration.

The octasubstituted long PEG chain macromonomers also decrease the cross-linking density as these macromonomers are of much higher molecular weight than those of shorter PEGs, which causes an increase in POSS−PEG content by weight. These changes in densities could be attributed to an increase in the porosity of the nanocomposites,[40,41] due to the increased free volume caused by very long PEG chains ($n = 6$) attached to the POSS cage. It is evident from Table 4 that for a significant increase in mol and wt % of POSS−PEG (up to 20 wt %) there is only slight increase in the POSS content. It appears that the actual wt % of POSS content is lower for the same mol % of two different chain length POSS−PEG. For example, the POSS cage content of 0.5 mol % POSS−PEG in hybrid materials for $[Q_8M_8^{(PEG)n=2}]$ and $[Q_8M_8^{(PEG)n=6}]$ is 5.5 and 4.6, respectively. Therefore, the presence of long PEG chain octasubstituted POSS cages, in the poly(methyl methacrylate) matrix, is likely to cause a decrease in the average cross-linking density, as a lower content of polymer chains is linked to the bulky octafunctional POSS cage. These have higher mobility caused by long PEG chains and a higher polymeric loading for a given mol % of cross-linker.

Conclusions

The incorporation of POSS−PEG macromonomers in the synthesis of hybrid organic−inorganic POSS-containing methacrylate-based polymers has been investigated. A series of cross-linked poly(methyl methacrylates) were prepared using various concentrations of methacryloyl-functional POSS (OMPS) nanosized cross-linking agent. The methacryloyl-functional POSS macromonomers were synthesized from our previously reported octafunctional POSS−PEG compounds by reaction with methacryloyl chloride. Octasubstituted methacryloyl-functional POSS cage structures were confirmed using various spectroscopy and thermal analyses, and the resultant materials were used as cross-linkers for the synthesis of three-component hybrid materials.

A series of different chain length OMPS macromonomers were used to synthesize a series of three-component hybrid materials, while varying the POSS concentrations. Materials containing 0.1−0.5 mol % of OMPS were prepared by polymerizing methyl methacrylate using benzoyl peroxide as a catalyst.

Thermal investigations using TGA and DSC techniques revealed that both POSS concentrations and PEG chain length play important roles in defining structure−property relationships. It would have been anticipated that the integration of multifunctionalized POSS into polymer matrices would enhance their glass transition temperatures.[42−47] However, in some cases, lower glass transition temperatures were realized upon the incorporation of POSS cages into the polymer structures.[48,49] Materials that have been prepared from longer chain POSS−PEG $[Q_8M_8^{PEG(n=6)}]$ as cross-linker showed a decrease in T_g in the hybrid, also observed in the DSC study. This was explained by the higher free volume induced by the presence of the bulky POSS−PEG in these three-component materials.

References and Notes

(1) Ray Ellsworth, M. W.; Gin, D. L. *Polym. News* **1999**, *24*, 331−341.
(2) Lau, K. T.; Hui, D. *Composites, Part B* **2002**, *33*, 263−277.
(3) Ray, S. S.; Okamoto, M. *Prog. Polym. Sci.* **2003**, *26*, 1539−1641.
(4) Li, G.; Wang, L.; Ni, H.; Pitman, C. U., Jr. *J. Inorg. Organomet. Polym.* **2001**, *11*, 123−154.

(5) Lichtenhan, J. D.; Otonary, Y. A.; Carr, M. J. *Macromolecules* **1995**, *28*, 8435−8437.
(6) Zheng, L.; Farris, R. J.; Coughlin, E. B. *Macromolecules* **2001**, *34*, 8034−8039.
(7) Hoflund, G. B.; Gonzales, R. I.; Phillips, S. H. *J. Adhes. Sci. Technol.* **2001**, *15*, 1199−1211.
(8) Harrison, P. G. *J. Organomet. Chem.* **1997**, *542*, 141−183.
(9) Voronkov, M. G.; Lavrent'yev, V. I. *Top. Curr. Chem.* **1982**, *102*, 199−236.
(10) Sellinger, A.; Laine, R. M. *Macromolecules* **1996**, *29*, 2327−2330.
(11) Zhang, C.; Laine, R. M. *J. Am. Chem. Soc.* **2000**, *122*, 6979−6988.
(12) Toepfer, O.; Neuman, D.; Choudhury, N. R.; Whittaker, A.; Matisons, J. *Chem. Mater.* **2005**, *17*, 1027−1035.
(13) Zhang, C.; Laine, R. M. *J. Organomet. Chem.* **1996**, *521*, 199−201.
(14) Sellinger, A.; Laine, R. M. *Chem. Mater.* **1996**, *8*, 1592−1593.
(15) Laine, R. M.; Choi, J.; Lee, I. *Adv. Mater.* **2001**, *13*, 800−803.
(16) Sellinger, A.; Laine, R. M.; Choi, J.; Costa, R. O. R. *Polym. Prepr.* **2000**, *41*, 524−525.
(17) Choi, J.; Harcup, J.; Yee, A. F.; Zhu, Q.; Laine, R. M. *J. Am. Chem. Soc.* **2001**, *123*, 11420−11430.
(18) Hoebel, D.; Pitsch, I.; Heidemann, D. *Z. Anorg. Allg. Chem.* **1990**, *538*, 133−144.
(19) Hoebel, D.; Pitsch, I.; Heidemann, D. *Z. Anorg. Allg. Chem.* **1991**, *592*, 207−216.
(20) Hoebel, D.; Endres, K.; Reinert, T.; Pitsch, I. *J. Non-Cryst. Solids* **1994**, *176*, 179−188.
(21) Harrison, P. G.; Kannengiesser, R. *Chem. Commun*. **1996**, 415−416.
(22) Zhang, C.; Babonneau, F.; Bonhomme, C.; Laine, R. M.; Soles, C. L.; Hristov, H. A.; Yee, A. F. *J. Am. Chem. Soc.* **1998**, *120*, 8380−8391.
(23) Tamaki, R.; Choi, J.; Laine, R. M. *Polym. Mater. Sci. Eng.* **2001**, *84*, 564−565.
(24) Tamaki, R.; Tanaka, Y.; Asuncion, M. Z.; Choi, J.; Laine, R. M. *J. Am. Chem. Soc.* **2001**, *123*, 12416−12417.
(25) Liu, H.; Zheng, S. *Macromol. Rapid Commun.* **2005**, *26*, 196−200.
(26) Markovic, E.; Ginic-Markovic, M.; Clarke, S.; Matisons, J.; Hussain, M.; Simon, G. P. *Macromolecules* **2007**, *40*, 2694−2701.
(27) Lichtenhan, J. D. *Comments Inorg. Chem.* **1995**, *17*, 115−130.
(28) Haddad, T. S.; Lichtenhan, J. D. *Macromolecules* **1996**, *29*, 7302−7304.
(29) Eisenberg, P.; Lucas, J. C.; Williams, R. J. *J. Macromol. Symp.* **2002**, *189*, 1−14.
(30) Liu, Y.; Meng, F.; Zheng, S. *Macromol. Rapid Commun.* **2005**, *26*, 920−925.
(31) Pebaron, P. C.; Wang, Z.; Pinnavia, T. J. *Appl. Clay Sci.* **1999**, *15*, 1−9.
(32) Ray, S. S.; Okamoto, M. *Prog. Polym. Sci.* **2003**, *28*, 1539−1641.
(33) Li, G. Z.; Wang, L.; Toghiani, H.; Daulton, T. L.; Koyama, K.; Pittman, C. U., Jr. *Macromolecules* **2001**, *34*, 8686−8693.
(34) Ni, Y.; Zheng, S.; Nie, K. *Polymer* **2004**, *45*, 5557−5568.
(35) Xu, H. Y.; Kuo, S. W.; Lee, J. S.; Chang, F. C. *Macromolecules* **2002**, *35*, 8788−8793.
(36) Haddad, T. S.; Lee, A.; Phillips, S. H. *Polym. Prepr.* **2001**, *42*, 88−89.
(37) Xu, H.; Kuo, S.-W.; Lee, J.-S.; Chang, F.-C. *Polymer* **2002**, *43*, 5117−5124.
(38) Kim, G. M.; Qin, H.; Fang, X.; Sun, F. C.; Mather, P. T. *J. Polym. Sci., Part B: Polym. Phys.* **2003**, *41*, 3299−3313.
(39) Wu, J.; Haddad, T. S.; Kim, G. M.; Mather, P. T. *Macromolecules* **2007**, *40*, 544−554.
(40) Leu, C.-M.; Chang, Y.-T.; Wei, K.-H.; Shu, C.-F. *Chem. Mater.* **2003**, *15*, 2261−2265.
(41) Leu, C.-M.; Chang, Y.-T.; Wei, K.-H. *Chem. Mater.* **2003**, *15*, 3721−3727.
(42) Lee, A.; Lichtenhan, J. D. *Macromolecules* **1998**, *31*, 4970−4974.
(43) Zhang, S.; Wang, J.; Guo, Q.; Wei, J.; Li, J. *Polymer* **1996**, *37*, 4667−4673.
(44) Mather, P. T.; Jeon, H. G.; Romo-Uribe, A.; Haddad, T. S.; Lichtenhan, J. D. *Macromolecules* **1999**, *32*, 1194−1203.
(45) Bharadwaj, R. K.; Berry, R. J.; Farmer, B. L. *Polymer* **2000**, *41*, 7209−7221.
(46) Lee, A.; Lichtenhan, J. D.; Reinerth, W. A. *Polym. Mater. Sci. Eng.* **2000**, *82*, 235−236.
(47) Xu, H. Y.; Kuo, S. W.; Lee, J. S.; Chang, F. C. *Macromolecules* **2002**, *35*, 8788−8793.
(48) Romo-Uribe, A.; Mather, P. T.; Haddad, T. S.; Lichtenhan, J. D. *J. Polym. Sci., Part B: Polym. Phys.* **1998**, *36*, 1857−1872.
(49) Abad, M. J.; Barral, L.; Fasce, D. F.; Williams, R. J. *Macromolecules* **2003**, *63*, 3128−3135.

MA702103Z